doi: 10.1103/PhysRevD.86.074514

Helium nuclei, deuteron, and dineutron in 2 + 1 flavor lattice QCD

Takeshi Yamazaki,[1,2] Ken-ichi Ishikawa,[2,3] Yoshinobu Kuramashi,[2,4,5] and Akira Ukawa[4]
[1]*Kobayashi-Maskawa Institute for the Origin of Particles and the Universe, Nagoya University, Naogya, Aichi 464-8602, Japan*
[2]*RIKEN Advanced Institute for Computational Science, Kobe, Hyogo 650-0047, Japan*
[3]*Department of Physics, Hiroshima University, Higashi-Hiroshima, Hiroshima 739-8526, Japan*
[4]*Center for Computational Sciences, University of Tsukuba, Tsukuba, Ibaraki 305-8577, Japan*
[5]*Graduate School of Pure and Applied Sciences, University of Tsukuba, Tsukuba, Ibaraki 305-8571, Japan*
(Received 18 July 2012; published 19 October 2012)

We calculate the binding energies for multinucleon bound states with the nuclear mass number less than or equal to 4 in 2 + 1 flavor QCD at the lattice spacing of $a = 0.09$ fm employing a relatively heavy quark mass corresponding to $m_\pi = 0.51$ GeV. To distinguish a bound state from attractive scattering states, we investigate the volume dependence of the energy shift between the ground state and the state of free nucleons by changing the spatial extent of the lattice from 2.9 to 5.8 fm. We conclude that ^{4}He, ^{3}He, deuteron and dineutron are bound at $m_\pi = 0.51$ GeV. We compare their binding energies with those in our quenched studies and also with several previous investigations.

DOI: 10.1103/PhysRevD.86.074514 PACS numbers: 11.15.Ha, 12.38.−t, 12.38.Aw, 12.38.Gc

I. INTRODUCTION

Lattice QCD has a potential ability to understand the nature of nuclei quantitatively, whose characteristic feature is a hierarchical structure in the strong interaction. The nuclear binding energy is experimentally known to be about 10 MeV per nucleon, which is much smaller than the typical energy scale of hadrons. A measurement of the binding energies is therefore the first step for direct investigation of nuclei in lattice QCD. A key ingredient in the study is a systematic change of the spatial volume of the lattice to distinguish a bound state from an attractive scattering state.

We carried out a first attempt to measure the binding energies of the ^{4}He and ^{3}He nuclei in quenched QCD with a rather heavy quark mass corresponding to $m_\pi = 0.80$ GeV, thereby avoiding a high computational cost [1]. We followed this work with a renewed investigation of the bound state for the two-nucleon channel in quenched QCD at the same quark mass, which found that not only the deuteron in the $^3S_1$ channel but also the dineutron in the $^1S_0$ channel is bound [2]. Independently, the NPLQCD Collaboration reported the possibility that a bound state is formed in both channels at $m_\pi = 0.39$ GeV in 2 + 1 flavor QCD [3]. They later confirmed the bound states for the helium nuclei and the two-nucleon channels at $m_\pi = 0.81$ GeV in 3-flavor QCD taking a different choice for the quark and gluon actions [4].

In this paper we report on our investigation of the dynamical quark effects on the binding energies of the helium nuclei, the deuteron and the dineutron. We perform a 2 + 1 flavor lattice QCD simulation with the degenerate up and down quark mass corresponding to $m_\pi = 0.51$ GeV. Four lattice sizes are employed to take the infinite spatial volume limit: $32^3 \times 48$, $40^3 \times 48$, $48^3 \times 48$ and $64^3 \times 64$, whose spatial extent ranges from 2.9 fm to 5.8 fm with the lattice spacing of $a = 0.08995(40)$ fm [5].

For the helium nuclei, our main interest lies in the magnitude of the binding energies since all studies carried out so far, both in quenched and in unquenched QCD and for several quark mass values, agree on the bound state nature for helium nuclei. Much more intriguing is the two-nucleon system, for which there are two ways to study. One is a direct investigation [2–4,6–9] in which one calculates the two-nucleon Green's functions directly in lattice QCD, and the other is an indirect calculation by means of the two-nucleon effective potential extracted from the two-nucleon wave function in lattice QCD [10,11].

So far only the former method has reported the binding energies of the two-nucleon systems. In quenched QCD the bound state nature has been confirmed for both channels at $m_\pi = 0.80$ GeV in our recent work [2]. On the other hand, unquenched studies show a complicated situation. A somewhat early study in 2 + 1 flavor QCD with a mixed action [8] reported a positive energy shift (repulsive interaction) in both channels at $m_\pi \leq 0.59$ GeV. More recently, however, deep bound states were observed at $m_\pi = 0.81$ GeV in 3-flavor QCD [4]. We hope to shed light on this situation with our own investigation in 2 + 1 flavor QCD.

This paper is organized as follows. In Sec. II we explain the simulation details including the simulation parameters and the interpolating operators for the multinucleon channels. Section III presents the results of the binding energies for the helium nuclei, the deuteron and the dineutron. We compare our results with those in the previous studies. Conclusions and discussions are summarized in Sec. IV.

II. SIMULATION DETAILS

A. Simulation parameters

We generate 2 + 1 flavor gauge configurations with the Iwasaki gauge action [12] and the nonperturbative

TABLE I. Simulation parameters for gauge configuration generation at $(\kappa_{ud}, \kappa_s) = (0.1373316, 0.1367526)$. The definition of parameters is the same as in Ref. [15].

$L^3 \times T$	$32^3 \times 48$	$40^3 \times 48$	$48^3 \times 48$	$64^3 \times 64$
# run	1	1	1	2
(N_0, N_1, N_2)	(2, 2, 10)	(2, 2, 15)	(2, 2, 16)	(2, 2, 18)
Block size	$8^3 \times 6$	$10^3 \times 6$	$12^2 \times 6^2$	$8^3 \times 4$
$N_{\rm poly}$	260	320	320	340
MD time	4000	2000	2000	(1090, 810)
$P_{\rm acc}$ (HMC)	0.840	0.925	0.916	(0.880, 0.867)
$P_{\rm acc}$ (GMP)	0.957	0.969	0.963	(0.978, 0.974)

$O(a)$-improved Wilson quark action at $\beta = 1.90$ with $c_{\rm SW} = 1.715$ [13]. The lattice spacing is $a = 0.8995(40)$ fm, corresponding to $a^{-1} = 2.194(10)$ GeV, determined with $m_\Omega = 1.6725$ GeV [5]. We take four lattice sizes, $L^3 \times T = 32^3 \times 48$, $40^3 \times 48$, $48^3 \times 48$ and $64^3 \times 64$, to investigate the spatial volume dependence of the ground state energy shift between the multinucleon system and the free nucleons. The physical spatial extents are 2.9, 3.6, 4.3, and 5.8 fm, respectively. Since it becomes harder to obtain a good signal-to-noise ratio at lighter quark masses for multinucleon systems [7,14], we employ the hopping parameters $(\kappa_{ud}, \kappa_s) = (0.1373316, 0.1367526)$ which correspond to $m_\pi = 0.51$ GeV and $m_N = 1.32$ GeV, and the physical value for the strange quark mass. These values are chosen based on the previous results for m_π and m_s obtained by the PACS-CS Collaboration [5,15].

We employ the domain-decomposed hybrid Monte Carlo algorithm [16,17] for the degenerate light quarks and the UV-filtered polynomial hybrid Monte Carlo algorithm [18] for the strange quark employing the Omelyan-Mryglod-Folk integrator [19,20]. The algorithmic details are given in Ref. [15]. We summarize the simulation parameters in Table I including the block sizes in domain-decomposed hybrid Monte Carlo and the polynomial order in UV-filtered polynomial hybrid Monte Carlo. We take $\tau = 1$ for the trajectory length of the molecular dynamics in all the runs. The step sizes are chosen such that we obtain reasonable acceptance rates presented in Table I. We generate the gauge configurations in a single run except for the $L = 64$ case for which we carry out two runs. The total trajectory length is about 2000 for all the volumes, except for the case of the smallest volume in which it is 4000.

B. Calculation method

We extract the ground state energies of the multinucleon systems and the nucleon state from the correlation functions

$$G_{\mathcal{O}}(t) = \langle 0|\mathcal{O}(t)\bar{\mathcal{O}}(0)|0\rangle, \tag{1}$$

with $\mathcal{O}$ being appropriate operators for ^{4}He, ^{3}He, two-nucleon $^3\mathrm{S}_1$ and $^1\mathrm{S}_0$ channels, and the nucleon state N (see the next subsection for actual expressions).

We carry out successive measurements in the interval of ten trajectories. The errors are estimated by jackknife analysis choosing 200 trajectories for the bin size for all volumes, except for the largest volume for which we use 190. The numbers of configurations are listed in Table II. We attempt to extract as much information as possible from each configuration by repeating the measurement of the correlation functions for a number of sources at different spatial points and time slices. For the 48^4 and 64^4 lattices, we calculate the correlation functions not only in the temporal direction but also in the three spatial directions exploiting the space-time rotational symmetry. We found that this procedure effectively increases statistics by a factor of 4. This factor is included in the number of measurements on each configuration given in Table II.

We are interested in the energy shift between the ground state of the multinucleon system and the free nucleons on an L^3 box,

$$\Delta E_L = E_{\mathcal{O}} - N_N m_N, \tag{2}$$

with $E_{\mathcal{O}}$ being the lowest energy level for the multinucleon channel, N_N the number of nucleon and m_N the nucleon mass. This quantity is directly extracted from the ratio of the multinucleon correlation function divided by the N_Nth power of the nucleon correlation function

$$R(t) = \frac{G_{\mathcal{O}}(t)}{(G_N(t))^{N_N}}, \tag{3}$$

where the same source operator is chosen for the numerator and the denominator. We also define the effective energy shift as

TABLE II. Number of configurations, separation of trajectories between each measurement, bin size in jackknife analysis, number of measurements on each configuration, exponential smearing parameter set (A, B) in Eq. (12), pion mass m_π and nucleon mass m_N are summarized for each lattice size.

L	T	# Config.	$\tau_{\rm sep}$	Bin size	# Meas.	(A, B)	m_π [GeV]	m_N [GeV]
32	48	200	20	10	192	(1.0, 0.18)	0.5109(16)	1.318(4)
40	48	200	10	20	192	(0.8, 0.22)	0.5095(8)	1.314(4)
48	48	200	10	20	192	(0.8, 0.23)	0.5117(9)	1.320(3)
64	64	190	10	19	256	(0.8, 0.23)	0.5119(4)	1.318(2)

$$\Delta E_L^{\rm eff} = \ln\left(\frac{R(t)}{R(t+1)}\right), \tag{4}$$

which is useful to check the plateau region in later sections.

Note that the definitions for ΔE_L and $\Delta E_L^{\rm eff}$ follow those in Ref. [2], but are opposite to those used in Ref. [1].

C. Interpolating operators

We use an interpolating operator for the proton given by

$$p_\alpha = \varepsilon_{abc}([u_a]^t C\gamma_5 d_b)u_c^\alpha, \tag{5}$$

where $C = \gamma_4\gamma_2$ and α and a, b, c are the Dirac index and the color indices, respectively. The neutron operator n_α is obtained by replacing u_c^α by d_c^α in the proton operator. To save on the computational cost we use the nonrelativistic quark operator in which the Dirac index is restricted to the upper two components.

The ^{4}He nucleus has zero total angular momentum, positive parity $J^P = 0^+$ and zero isospin $I = 0$. We employ the simplest ^{4}He interpolating operator with zero orbital angular momentum $L = 0$, and hence $J = S$ with S being the total spin. Such an operator was already given a long time ago in Ref. [21],

$$^4{\rm He} = \frac{1}{\sqrt{2}}(\bar\chi\eta - \chi\bar\eta), \tag{6}$$

where

$$\chi = \frac{1}{2}([+-+-] + [-+-+] - [+--+] - [-++-]), \tag{7}$$

$$\bar\chi = \frac{1}{\sqrt{12}}([+-+-] + [-+-+] + [+--+] + [-++-] - 2[++--] - 2[--++]), \tag{8}$$

with $+/-$ being the up/down spin of each nucleon, and η, $\bar\eta$ are obtained by replacing $+/-$ in χ, $\bar\chi$ by p/n for the isospin. Each nucleon in the sink operator is projected to zero spatial momentum.

We also calculate the correlation function of the ^{3}He nucleus whose quantum numbers are $J^P = \frac{1}{2}^+$, $I = \frac{1}{2}$ and $I_z = \frac{1}{2}$. We employ the interpolating operator in Ref. [22],

$$^3{\rm He} = \frac{1}{\sqrt{6}}(|p_-n_+p_+\rangle - |p_+n_+p_-\rangle + |n_+p_+p_-\rangle - |n_+p_-p_+\rangle + |p_+p_-n_+\rangle - |p_-p_+n_+\rangle), \tag{9}$$

with the zero momentum projection on each nucleon in the sink operator.

The two-nucleon operators for the ^{3}S$_1$ and ^{1}S$_0$ channels are given by

$$NN_{^3{\rm S}_1}(t) = \frac{1}{\sqrt{2}}[p_+(t)n_+(t) - n_+(t)p_+(t)], \tag{10}$$

$$NN_{^1{\rm S}_0}(t) = \frac{1}{\sqrt{2}}[n_+(t)n_-(t) - n_-(t)n_+(t)]. \tag{11}$$

In the spin triplet channel the operators for the other two spin components are constructed in a similar way. We take the average over the three spin components.

The quark propagators are solved with the periodic boundary condition in all the spatial and temporal directions using the exponentially smeared source of form

$$q'(\vec x, t) = \sum_{\vec y} A e^{-B|\vec x - \vec y|} q(\vec y, t) \tag{12}$$

after the Coulomb gauge fixing. We choose the smearing parameters depending on the volume (see Table II) in order to obtain reasonable plateaus of the effective energy for the ground states in the multinucleon channels as well as for the nucleon. For the source operators explained above we insert the *smeared* quark fields of Eq. (12) for each nucleon operator located at the same spatial point $\vec x$. Each nucleon in the sink operator, on the other hand, is composed of the *point* quark fields, and projected to zero spatial momentum.

D. Difficulties for multinucleon channel

There are several computational difficulties in the calculation of the correlation functions $G_{\mathcal{O}}(t)$ for the ^{3}He and ^{4}He channels. One is a factorially large number of Wick contractions for the quark-antiquark fields. A naive counting gives $(2N_p + N_n)!(2N_n + N_p)!$ for a nucleus composed of N_p protons and N_n neutrons, which quickly becomes prohibitively large beyond three-nucleon systems, e.g., 2880 for ^{3}He and 518400 for ^{4}He. To overcome the difficulty, we use the reduction techniques proposed in our exploratory work [1]. After the reduction, only 1107 (93) contractions are required for the correlation function in the ^{4}He (^{3}He) channel. Other reduction techniques for the large number of the Wick contractions have been proposed for the multimeson [23] and multibaryon [24,25] channels.

Another difficulty in studying a multinucleon bound state is the identification of the bound state nature in a finite volume because an attractive scattering state yields a similar energy shift due to the finite volume effect [26–28]. To solve the problem we need to investigate the volume dependence of the measured energy shift [1,2]: For a scattering state, the energy shift decreases in proportion to $1/L^3$ at the leading order in the $1/L$ expansion [26,29], while for a bound state the energy shift remains at a finite value in the infinite spatial volume limit. In order to distinguish a nonzero constant from a $1/L^3$ behavior in the energy shift, we employ four spatial extents from 2.9 to 5.8 fm.

Furthermore, when the mass number increases we need to consider the possibility of multinuclei states such as the two-deuteron state in the ^{4}He channel. In the present work we simply calculate only the energy shift of the ground state from the free multinucleon state, but we will briefly comment on this problem in Sec. IV.

III. RESULTS

A. Nucleon

We first show the effective nucleon mass on the $(5.8\ \mathrm{fm})^3$ box in Fig. 1 as a typical result. The plateau of the effective mass is clearly observed. A fit result of the correlation function with an exponential form is also drawn in the figure with the one standard deviation error band. We list the nucleon mass together with the pion mass in Table II.

B. ^{4}He nucleus

The effective energy shift $\Delta E_L^{\mathrm{eff}}$ defined in Eq. (4) is plotted in Fig. 2. The signal is clear up to $t = 12$, beyond which the statistical error increases rapidly. The energy shift ΔE_L is extracted from $R(t)$ of Eq. (3) by an exponential fit over the range of $t = 10$–14. The fit result is denoted by the solid lines with the statistical error band in Fig. 2. The systematic error in the fit is estimated from the variation of the fit results with the minimum or maximum time slice changed by ± 1. Results with similar quality are obtained on other volumes. We summarize the values of ΔE_L with the statistical and systematic errors in Table III.

Figure 3 shows the volume dependence of ΔE_L as a function of $1/L^3$. The inner bar denotes the statistical error and the outer bar represents the statistical and systematic errors combined in quadrature. The negative energy shifts are obtained in all the four volumes. We extrapolate the results to the infinite volume limit with a simple linear function of $1/L^3$,

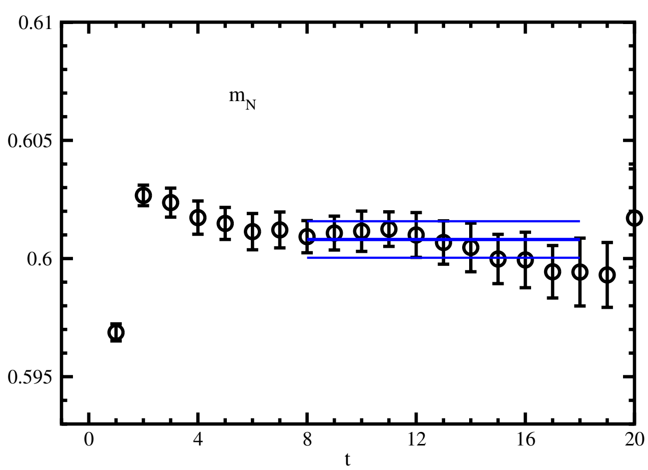

FIG. 1 (color online). Nucleon effective mass on the $(5.8\ \mathrm{fm})^3$ box in lattice units. Fit result with one standard deviation error band is expressed by solid lines.

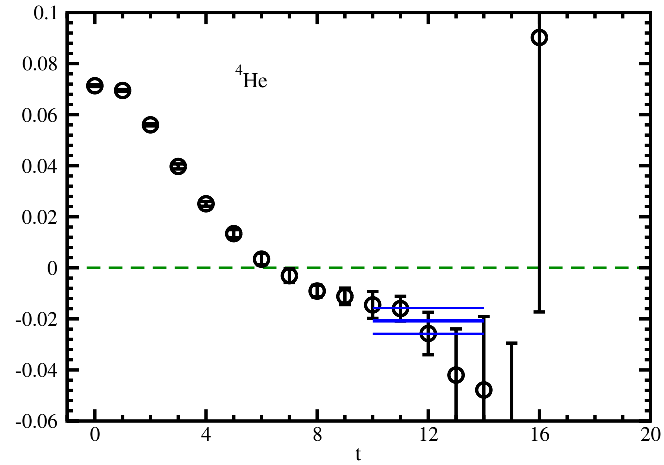

FIG. 2 (color online). Effective energy shift $\Delta E_L^{\mathrm{eff}}$ for the ^{4}He channel on the $(5.8\ \mathrm{fm})^3$ box in lattice units. Fit result with one standard deviation error band is expressed by solid lines.

$$\Delta E_L = \Delta E_\infty + \frac{C_L}{L^3}. \tag{13}$$

The systematic error is estimated from the variation of the results obtained by alternative fits which contain a constant fit of the data obtained with a different fit range in t. The nonzero negative value obtained for the infinite volume limit ΔE_∞ shown in Fig. 3 and Table III leads us to conclude that the ground state is bound in this channel for the quark masses employed. The binding energy $-\Delta E_\infty = 43(12)(8)$ MeV, where the first error is statistical and the second one is systematic, is consistent with the experimental result of 28.3 MeV and also with the previous quenched result at $m_\pi = 0.80$ GeV [2]. Note that the error is still quite large.

A recent work in 3-flavor QCD at $m_\pi = 0.81$ GeV reported a value 110(20)(15) MeV for the binding energy of the ^{4}He nucleus [4]. This is about three times deeper than our value. Whether this difference can be attributed to the quark mass dependence in unquenched calculations needs to be clarified in the future.

TABLE III. Energy shift $-\Delta E_L$ in physical units and fit range for the ^{4}He and ^{3}He channels on each spatial volume. Extrapolated results in the infinite spatial volume limit are also presented. The first and second errors are statistical and systematic, respectively.

	^{4}He		^{3}He	
L	$-\Delta E_L$ [MeV]	Fit range	$-\Delta E_L$ [MeV]	Fit range
32	47(24)(5)	10–14	23.2(7.6)(1.4)	10–14
40	30(15)(23)	9–13	20.2(6.9)(2.8)	9–14
48	39(20)(27)	10–14	25.5(5.3)(1.7)	10–14
64	46(11)(8)	10–14	19.5(3.7)(1.2)	9–14
∞	43(12)(8)	⋯	20.3(4.0)(2.0)	⋯

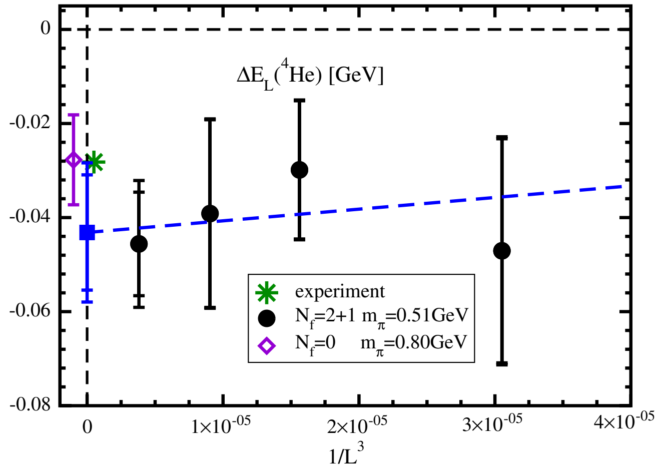

FIG. 3 (color online). Spatial volume dependence of ΔE_L in GeV units for the ^{4}He channel. Outer bar denotes the combined error of statistical and systematic ones added in quadrature. Inner bar is for the statistical error. Extrapolated result in the infinite spatial volume limit is shown by filled square symbol together with the fit line (dashed). Experimental value (star) and quenched result (open diamond) are also presented.

C. ^{3}He nucleus

Figure 4 shows the effective energy shift $\Delta E_L^{\mathrm{eff}}$ of Eq. (4). The quality of the signal is better than the ^{4}He channel in Fig. 2. An exponential fit of $R(t)$ in Eq. (3) with the range of $t = 9$–14 yields a negative value, which is denoted by the solid lines with the statistical error band in Fig. 4. The systematic error in the fit is estimated in the same way as in the ^{4}He case.

As listed in Table III, we find nonzero negative values for the energy shift ΔE_L for all the volumes. The volume dependence is illustrated in Fig. 5 as a function of $1/L^3$ with the inner and outer error bars as explained in the previous subsection. We carry out a linear extrapolation of Eq. (13). The systematic error is estimated in the same

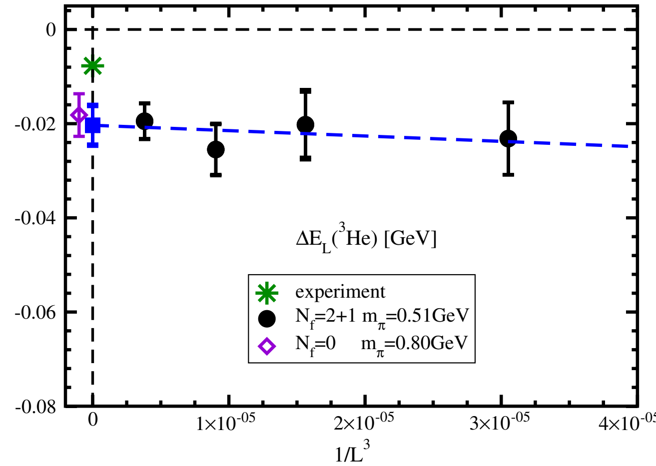

FIG. 5 (color online). Same as Fig. 3 for the ^{3}He channel.

way as in the ^{4}He channel. The energy shift extrapolated to the infinite spatial volume limit is nonzero and negative (see Fig. 5 and Table III), which means that the ground state is a bound state in this channel. The value of $-\Delta E_\infty = 20.3(4.0)(2.0)$ MeV is roughly three times larger than the experimental result, 7.72 MeV, though consistent with our previous quenched result at $m_\pi = 0.80$ GeV [2].

In 3-flavor QCD, $-\Delta E_\infty = 71(6)(5)$ MeV was reported [4] at a heavier quark mass corresponding to $m_\pi = 0.81$ GeV. Here again future work is needed to see if a quark mass dependence explains the difference from the experiment.

D. Two-nucleon channels

1. Present work

In Fig. 6 we show the time dependence for $\Delta E_L^{\mathrm{eff}}$ of Eq. (4) in the ${}^3S_1$ channel. The signals are lost beyond $t \approx 14$. We observe negative values beyond the error bars in the plateau region of $t = 9$–14. We extract the value of

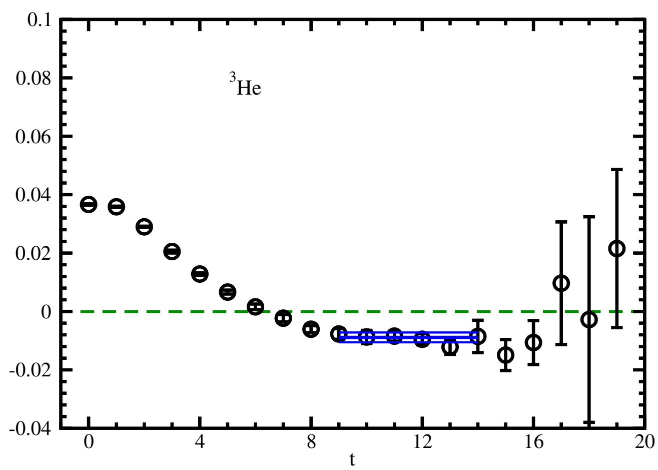

FIG. 4 (color online). Same as Fig. 2 for the ^{3}He channel.

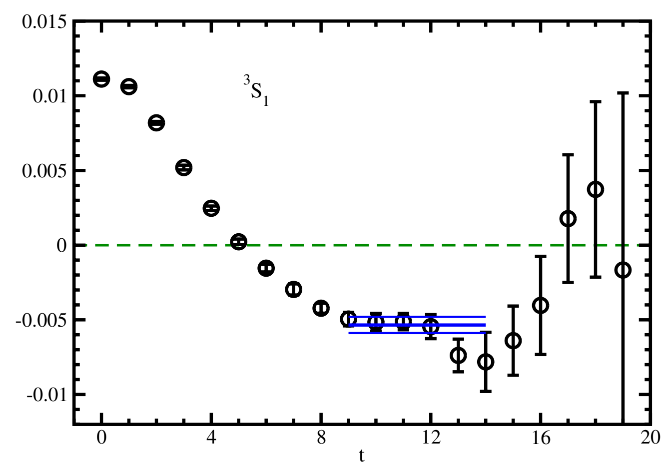

FIG. 6 (color online). Same as Fig. 2 for the ${}^3S_1$ channel.

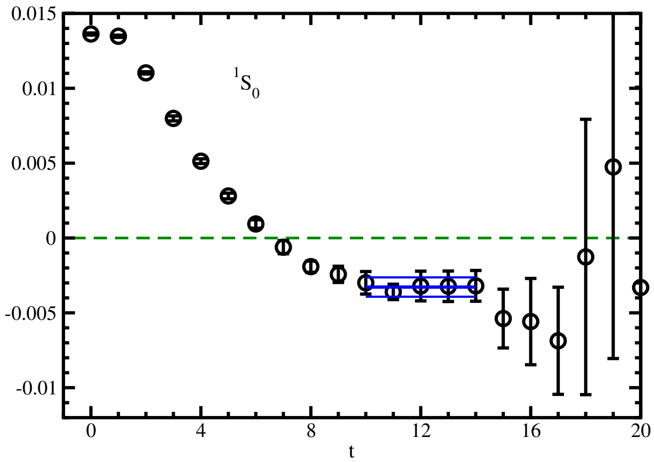

FIG. 7 (color online). Same as Fig. 2 for the $^1S_0$ channel.

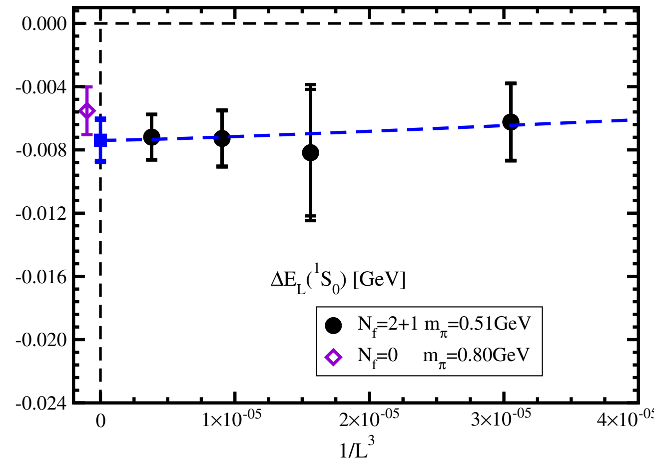

FIG. 9 (color online). Same as Fig. 3 for the $^1S_0$ channel.

ΔE_L from an exponential fit for $R(t)$ of Eq. (3) in the range of $t = 9$–14. The systematic error of the fit is estimated as explained in the previous subsections.

Figure 7 shows the result for $\Delta E_L^{\rm eff}$ in the $^1S_0$ channel on the (5.8 fm)^3 box. The value of $\Delta E_L^{\rm eff}$ is again negative beyond the error bars in the plateau region, though the absolute value is smaller than in the $^3S_1$ case. The energy shift ΔE_L is obtained in the same way as for the $^3S_1$ channel.

The volume dependences of ΔE_L in the $^3S_1$ and $^1S_0$ channels are plotted as a function of $1/L^3$ in Figs. 8 and 9, respectively. The numerical values of ΔE_L on all the spatial volumes are summarized in Table IV, where the statistical and systematic errors are given in the first and second parentheses, respectively. There is little volume dependence for ΔE_L, indicating a nonzero negative value in the infinite volume and a bound state, rather than the $1/L^3$ dependence expected for a scattering state, for the ground state for both channels.

The binding energies in the infinite spatial volume limit in Table IV are obtained by fitting the data with a function including a finite volume effect on the two-particle bound state [27,28],

$$\Delta E_L = -\frac{\gamma^2}{m_N}\left\{1 + \frac{C_\gamma}{\gamma L}\sum_{\vec{n}}{}' \frac{\exp(-\gamma L\sqrt{\vec{n}^2})}{\sqrt{\vec{n}^2}}\right\}, \quad (14)$$

where γ and C_γ are free parameters, $\vec{n}$ is a three-dimensional integer vector and $\sum'_{\vec{n}}$ denotes the summation without $|\vec{n}| = 0$. The binding energy $-\Delta E_\infty$ is determined from

$$-\Delta E_\infty = \frac{\gamma^2}{m_N}, \quad (15)$$

where we assume

$$2\sqrt{m_N^2 - \gamma^2} - 2m_N \approx -\frac{\gamma^2}{m_N}. \quad (16)$$

The systematic error is estimated from the variation of the fit results choosing different fit ranges in the determination of ΔE_L and also using constant and linear fits as alternative fit forms. We obtain the binding energies $-\Delta E_\infty = 11.5(1.1)(0.6)$ MeV and 7.4(1.3)(0.6) MeV for the $^3S_1$ and $^1S_0$ channels, respectively. The result for the $^3S_1$ channel is roughly five times larger than the experimental value, 2.22 MeV. Our finding of a bound state in the $^1S_0$ channel contradicts the experimental observation.

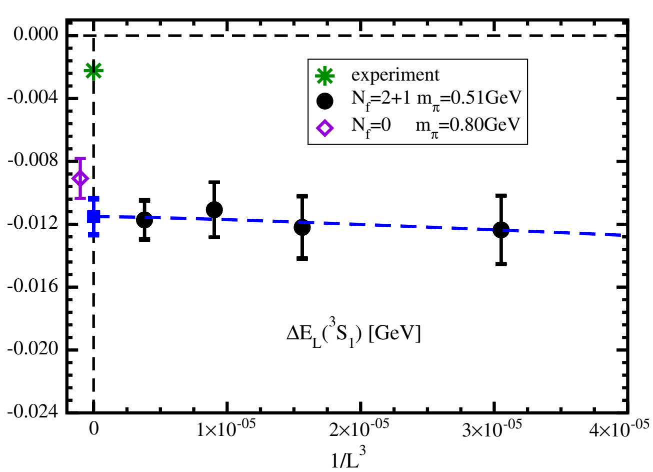

FIG. 8 (color online). Same as Fig. 3 for the $^3S_1$ channel.

TABLE IV. Same as Table III for the $^3S_1$ and $^1S_0$ channels.

	$^3S_1$		$^1S_0$	
L	$-\Delta E_L$ [MeV]	Fit range	$-\Delta E_L$ [MeV]	Fit range
32	12.4(2.1)(0.5)	9–14	6.2(2.4)(0.5)	10–14
40	12.2(1.9)(0.6)	10–15	8.2(4.0)(1.5)	11–15
48	11.1(1.7)(0.3)	10–14	7.3(1.7)(0.5)	10–14
64	11.7(1.2)(0.5)	9–14	7.2(1.4)(0.3)	10–14
∞	11.5(1.1)(0.6)	...	7.4(1.3)(0.6)	...

These features are consistent with our quenched results with a heavy quark mass corresponding to $m_\pi = 0.80$ GeV [2].

2. Comparison with previous studies

A number of studies have been performed for the two-nucleon channel after the first work of Ref. [7]. It is therefore instructive to summarize the results and make a comparison with each other. Table V tabulates in chronological order the results for $-\Delta E_L$ for the $^3\mathrm{S}_1$ and $^1\mathrm{S}_0$ channels together with the pion mass m_π and the spatial extent L in physical units. The numbers are plotted in Figs. 10 and 11 for the $^3\mathrm{S}_1$ and $^1\mathrm{S}_0$ channels, respectively, as a function of m_π^2.

The early studies in Refs. [7,8,11] employed a single volume, and we do not observe a common feature or trend among them. The positive values for $-\Delta E_L$ in Ref. [8] mean repulsive interaction for both channels, which is not seen in other studies. The results for $-\Delta E_L$ in Ref. [11] is an order of magnitude smaller compared to other groups, probably due to significant contamination from excited states.

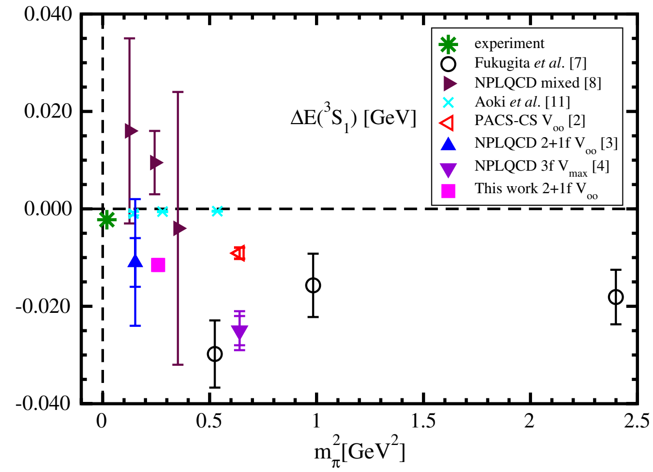

FIG. 10 (color online). m_π^2 dependence of ΔE_∞ for the $^3\mathrm{S}_1$ channel. Closed (open and cross) symbol denote the $2+1/3$ flavor (quenched) result. The results of Refs. [2,3] and this work are extrapolated values in the infinite volume limit. Experimental result (star) is also presented for comparison.

TABLE V. Energy shift $-\Delta E_L$ in physical units for the $^3\mathrm{S}_1$ and $^1\mathrm{S}_0$ channels together with the previous works. The values marked by * are estimated from the scattering length in Ref. [8] employing the leading term of finite volume formula in the $1/L$ expansion [26] with the nucleon mass obtained from the same ensemble in Ref. [30]. The values for Ref. [2] are taken from the results with the $\mathcal{O}_1$ interpolating operator.

Ref.	Quark action	# Flavor	m_π [GeV]	L [fm]	$-\Delta E_L$ [MeV] $^3\mathrm{S}_1$	$^1\mathrm{S}_0$
[7]	Wilson	0	0.72	2.7	29.8(6.9)	14.7(4.3)
		0	0.99	2.7	15.7(6.5)	10.7(4.3)
		0	1.55	2.7	18.1(5.6)	12.2(3.9)
[8]	Mixed (DW on Asqtad)	2 + 1	0.35	2.5	−16(19)*	−16(13)*
		2 + 1	0.49	2.5	−9.5(6.5)*	−15.1(4.2)*
		2 + 1	0.59	2.5	0.4(2.8)*	0.0(1.1)*
[11]	Wilson	0	0.38	4.4	0.97(37)	0.68(26)
		0	0.53	4.4	0.56(11)	0.509(94)
		0	0.73	4.4	0.480(97)	0.400(83)
[2]	Wilson-clover	0	0.80	3.1	10.2(2.2)(1.6)	6.1(2.3)(2.2)
		0	0.80	6.1	9.6(2.6)(0.9)	5.2(2.6)(0.8)
		0	0.80	12.3	7.8(2.1)(0.4)	4.6(2.0)(1.1)
		0	0.80	∞	9.1(1.1)(0.5)	5.5(1.1)(1.0)
[9]	Aniso. Wilson-clover	2 + 1	0.39	2.4	1.6(2.6)(4.3)	3.9(1.7)(2.6)
[3]	Aniso. Wilson-clover	2 + 1	0.39	3.0	22.3(2.3)(5.4)	10.4(2.6)(3.1)
		2 + 1	0.39	3.9	14.9(2.3)(5.8)	8.3(2.2)(3.3)
		2 + 1	0.39	∞	11(5)(12)	7.1(5.2)(7.3)
[4]	Stout Wilson-clover	2 + 1	0.81	3.4	25(3)(2)	16(3)(1)
		2 + 1	0.81	4.5	21(3)(1)	11(2)(1)
		2 + 1	0.81	6.7	25(3)(2)	19(3)(1)
This work	Wilson-clover	2 + 1	0.51	2.9	12.4(2.1)(0.5)	6.2(2.4)(0.5)
		2 + 1	0.51	3.6	12.2(1.9)(0.6)	8.2(4.0)(1.5)
		2 + 1	0.51	4.3	11.1(1.7)(0.3)	7.3(1.7)(0.5)
		2 + 1	0.51	5.8	11.7(1.2)(0.5)	7.2(1.4)(0.3)
		2 + 1	0.51	∞	11.5(1.1)(0.6)	7.4(1.3)(0.6)

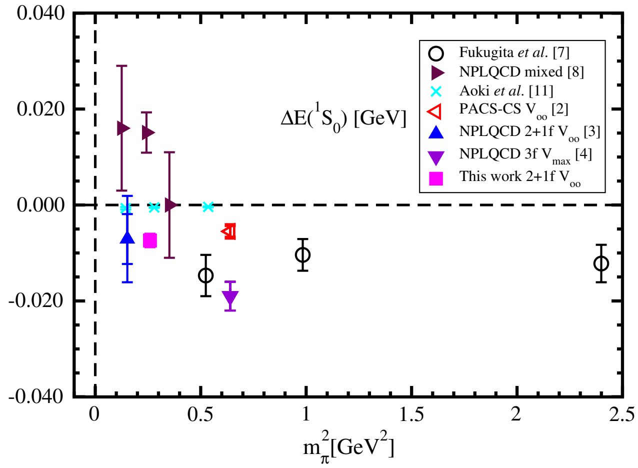

FIG. 11 (color online). Same as Fig. 10 for the $^1S_0$ channel.

The four recent studies [2–4] have made a systematic investigation of the spatial volume dependence. Our quenched and 2 + 1 flavor results show qualitatively the same feature that the binding energy for the $^3S_1$ channel is much larger than the experimental value and the bound state is observed in the $^1S_0$ channel. The 2 + 1 flavor results from Refs. [3,4] at $m_\pi = 0.39$ GeV give nonzero negative values for ΔE_L in both channels on the $\leq (3.9\ \mathrm{fm})^3$ box, which are consistent with our results as shown in Table V. Unfortunately, the extrapolation to the infinite spatial volume limit introduces large errors so that ΔE_∞ becomes consistent with zero within the error bars. The most recent study [4] worked at a heavier quark mass of $m_\pi =$ 0.81 GeV in 3-flavor QCD and found large values for the binding energies: 25(3)(2) MeV for the $^3S_1$ channel and 19(3)(1) MeV for the $^1S_0$ channel [4]. While all recent studies are consistent with a bound ground state for both $^3S_1$ and $^1S_0$ channels when quark masses are heavy, quantitative details still need to be clarified.

IV. CONCLUSION AND DISCUSSION

We have calculated the binding energies for the helium nuclei, the deuteron and the dineutron in 2 + 1 flavor QCD with $m_\pi = 0.51$ GeV and $m_N = 1.32$ GeV. The bound states are distinguished from the attractive scattering states by investigating the spatial volume dependence of the energy shift ΔE_L. In the infinite spatial volume limit we obtain

$$-\Delta E_\infty = \begin{cases} 43(12)(8) & \text{MeV for } ^4\text{He}, \\ 20.3(4.0)(2.0) & \text{MeV for } ^3\text{He}, \\ 11.5(1.1)(0.6) & \text{MeV for } ^3\text{S}_1, \\ 7.4(1.3)(0.6) & \text{MeV for } ^1\text{S}_0. \end{cases} \qquad (17)$$

In the present work we have discussed only the energy shift of the nucleus from the free multinucleon state, but there are other states we need to distinguish when the mass number increases, e.g., the two-deuteron state in the ^{4}He channel. The distinction of the ^{4}He nucleus from the two-deuteron state is less clear than the case with the four-nucleon state since the relative energy shift $\Delta E_\infty(^4\mathrm{He}) - 2\Delta E_\infty(^3\mathrm{S}_1) = -19(13)$ MeV is away from zero in less than 1.5 standard deviations due to large statistical error. The situation could be improved by increasing statistics.

While the binding energy for the ^{4}He nucleus is comparable with the experimental value, those for the ^{3}He nucleus and the deuteron are much larger than the experimental ones. Furthermore, we detect the bound state in the $^1S_0$ channel as in the previous study with quenched QCD, which is not observed in nature. These findings and the enhanced binding energies at $m_\pi = 0.81$ GeV in 3-flavor QCD [4] tell us that a next step of primary importance is to reduce the up-down quark mass toward the physical values. A possible scenario in the two-nucleon channels is as follows. The binding energy in both channels diminishes monotonically as the up-down quark mass decreases. At some point of the up-down quark mass the binding energy in the $^1S_0$ channel vanishes and the bound state evaporates into the attractive scattering state, while the binding energy in the $^3S_1$ channel remains finite up to the physical point. This is a dynamical question on the strong interaction, and only lattice QCD could answer it.

ACKNOWLEDGMENTS

Numerical calculations for the present work have been carried out on the HA8000 cluster system at the Information Technology Center of the University of Tokyo, on the PACS-CS computer under the "Interdisciplinary Computational Science Program" and the HA-PACS system under the HA-PACS Project for advanced interdisciplinary computational sciences by the exascale computing technology of the Center for Computational Sciences at the University of Tsukuba, on the T2K-Tsukuba cluster system at the University of Tsukuba, and on the K computer at the RIKEN Advanced Institute for Computational Science. We thank our colleagues in the PACS-CS Collaboration for helpful discussions and for providing us the code used in this work. This work is supported in part by Grants-in-Aid for Scientific Research from the Ministry of Education, Culture, Sports, Science and Technology (Grants No. 18104005, No. 18540250 and No. 22244018), and Grants-in-Aid of the Japanese Ministry for Scientific Research on Innovative Areas (Grants No. 20105002, No. 21105501 and No. 23105708).

[1] T. Yamazaki, Y. Kuramashi, and A. Ukawa (PACS-CS Collaboration), Phys. Rev. D **81**, 111504 (2010).
[2] T. Yamazaki, Y. Kuramashi, and A. Ukawa, Phys. Rev. D **84**, 054506 (2011).
[3] S. Beane, E. Chang, W. Detmold, H. Lin, T. Luu, K. Orginos, A. Parreño, M. Savage, A. Torok, and A. Walker-Loud (NPLQCD Collaboration), Phys. Rev. D **85**, 054511 (2012).
[4] S. Beane *et al.* (NPLQCD Collaboration), arXiv:1206.5219.
[5] S. Aoki *et al.* (PACS-CS Collaboration), Phys. Rev. D **81**, 074503 (2010).
[6] M. Fukugita, Y. Kuramashi, H. Mino, M. Okawa, and A. Ukawa, Phys. Rev. Lett. **73**, 2176 (1994).
[7] M. Fukugita, Y. Kuramashi, M. Okawa, H. Mino, and A. Ukawa, Phys. Rev. D **52**, 3003 (1995).
[8] S. R. Beane, P. F. Bedaque, K. Orginos, and M. J. Savage, Phys. Rev. Lett. **97**, 012001 (2006).
[9] S. R. Beane, W. Detmold, H.-W. Lin, T. C. Luu, K. Orginos, M. J. Savage, A. Torok, and A. Walker-Loud (NPLQCD Collaboration), Phys. Rev. D **81**, 054505 (2010).
[10] N. Ishii, S. Aoki, and T. Hatsuda, Phys. Rev. Lett. **99**, 022001 (2007).
[11] S. Aoki, T. Hatsuda, and N. Ishii, Prog. Theor. Phys. **123**, 89 (2010).
[12] Y. Iwasaki, arXiv:1111.7054.
[13] S. Aoki *et al.* (CP-PACS and JLQCD Collaborations), Phys. Rev. D **73**, 034501 (2006).
[14] G. P. Lepage, Reports No. CLNS-89-971 and C89-06-04, 1989.
[15] S. Aoki *et al.* (PACS-CS Collaboration), Phys. Rev. D **79**, 034503 (2009).
[16] M. Lüscher, J. High Energy Phys. 05 (2003) 052.
[17] M. Lüscher, Comput. Phys. Commun. **165**, 199 (2005).
[18] K.-I. Ishikawa *et al.* (PACS-CS Collaboration), Proc. Sci., LAT2006 (2006) 027.
[19] I. P. Omelyan, I. M. Mryglod, and R. Folk, Comput. Phys. Commun. **151**, 272 (2003).
[20] T. Takaishi and P. de Forcrand, Phys. Rev. E **73**, 036706 (2006).
[21] J. E. Beam, Phys. Rev. **158**, 907 (1967).
[22] M. Bolsterli and E. Jezak, Phys. Rev. **135**, B510 (1964).
[23] W. Detmold and M. J. Savage, Phys. Rev. D **82**, 014511 (2010).
[24] T. Doi and M. G. Endres, arXiv:1205.0585 [Comput. Phys. Commun. (to be published)].
[25] W. Detmold and K. Orginos, arXiv:1207.1452.
[26] M. Lüscher, Commun. Math. Phys. **105**, 153 (1986).
[27] S. R. Beane, P. F. Bedaque, A. Parreno, and M. J. Savage, Phys. Lett. B **585**, 106 (2004).
[28] S. Sasaki and T. Yamazaki, Phys. Rev. D **74**, 114507 (2006).
[29] S. R. Beane, W. Detmold, and M. J. Savage, Phys. Rev. D **76**, 074507 (2007).
[30] J. Bratt *et al.* (LHPC Collaboration), Phys. Rev. D **82**, 094502 (2010).